63-3-4

MASSACHUSETTS INSTITUTE OF TECHNOLOGY
METALS PROCESSING LABORATORY

THE STRENGTH AND PLASTICITY OF ANISOTROPIC METALS

Technical Report WAL TR 834.12/2-1

by

W. A. Backofen

and

W. F. Hosford, Jr.

31 December 1962

Second Quarterly Report

Contract DA-19-020-ORD-5719
Boston Procurement District

Ordnance Management Structure Code 5010.11.8430051
Department of the Army Project 59332008
U. S. Army Materials Research Agency
Watertown 72, Massachusetts

Cambridge, Massachusetts

The findings in this report are not to be construed as an official Department of the Army position.

ASTIA AVAILABILITY NOTICE

Qualified requesters may obtain copies of this report from ASTIA.

Disposition Instructions

Destroy; do not return.

AD NO._____

Plastic deformation
Plasticity
Stress and strain

THE STRENGTH AND PLASTICITY OF ANISOTROPIC METALS

Technical Report WAL TR 834.12/2-1

by

W. A. Backofen

and

W. F. Hosford, Jr.

31 December 1962

Second Quarterly Report

Contract DA-19-020-ORD-5719
Boston Procurement District

Ordnance Management Structure Code 5010.11.8430051
Department of the Army Project 59332008
U. S. Army Materials Research Agency
Watertown 72, Massachusetts

Cambridge, Massachusetts

Abstract

Tension tests have been made on strip specimens cut at different angles from textured sheets. For a pure titanium sheet, RC-70 annealed, the angular variation of yield stress and strain ratio do not agree with the predictions of Hill's anisotropic plasticity theory. Relatively low R values observed in magnesium alloy (AZ31B) sheets with strong (0001) textures are interpreted as resulting from basal slip.

For cubic metals, a method is outlined for calculating the relationship of plastic anisotropy to crystallographic texture. The method, which is an extension of Taylor's analysis of plastic strains in polycrystalline metals, is used to predict the flow stress and strain ratio resulting from various textures.

Experimental Work on Textured Sheets of HCP Metals

Tension tests have been made on strip specimens cut from textured sheets at different angles to the reference (rolling and transverse) directions. The purpose was to check the anisotropic plasticity theory of Hill,[1] which makes predictions about the angular variation of yield stress and strain ratio.

Early in the testing program it became apparent that micrometer measurements to determine width strains for calculation of strain ratios led to a large experimental scatter. Small width variations from place to place because of machining irregularities or development of an "orange-peel" surface texture caused substantial variations in calculated strains. To avoid this difficulty, a travelling microscope was subsequently used to measure the width dimension between fixed gage points.

The results of tests on a 0.067-in.-thick sheet of commerically pure titanium (RC-70 annealed) are shown in Fig. 1. The variation of yield stress σ, with angle of testing is almost linear, the maximum occurring at 90° (the transverse direction) and the minimum at 0° (the rolling direction). The variation of the strain ratio R, is not so straightforward, however, with minima occurring at 0 and 90° and a maximum near 60°.

According to the theory,

$$\sigma = \left[F_{\sin}{}^2 \alpha + G \cos^2 \alpha + H + (2N-F-G-4H) \sin^2 \alpha \cos^2 \alpha \right]^{-1/2} \qquad (1)$$

and

$$R = \frac{H + (2N-F-G-4H) \sin^2 \alpha \cos^2 \alpha}{F \sin^2 \alpha + G \cos^2 \alpha} \qquad (2)$$

where σ is the yield stress, R the strain ratio, and α the angle between the strip axis and the rolling direction. H, N, F, and G are anisotropy parameters of the material. When the measured strain ratios from Fig. 1 are substituted into Eq. 2, it is found that

at	$\alpha = 0^\circ$	G/H = 2.0	
	$\alpha = 90^\circ$	F/H = 0.96	
	$\alpha = 22\text{-}1/2^\circ$	N/H = 6.5	(using G/H = 2.0; F/H = 0.96)
	$\alpha = 45^\circ$	N/H = 6.4	(" " ")
	$\alpha = 67\text{-}1/2^\circ$	N/H = 12.3	(" " ")

With G/H = 2.0 and F/H = 0.96, Eq. 1 predicts a yield-stress minimum between $\alpha = 0$ and $\alpha = 90^{\circ}$ for any value of $N/H > 4.0$. The wide range of calculated N/H values and the absence of a yield-stress minimum clearly show that the data are not consistent with the Hill analysis. The difficulty may lie in the basic assumption that the sheet normal is an axis of two-fold, four-fold or rotational symmetry. Textural components with six-fold symmetry may be present in this and other sheets of HCP materials and thus contribute to the disagreement between theory and experiment.

Transverse and longitudinal tension tests were also made on a magnesium alloy AZ31B in both the hard (H-24) and soft (O) tempers, with results given in the table. In every test the R values increased markedly with strain.

Temper	Testing Direction	Strain Ratio R at axial strain of 1%	10%
H-24	Rolling	0.38	1.00
H-24	Transverse	1.76	2.89
O	Rolling	0.58	1.28
O	Transverse	1.56	3.04

The (0001) pole figures supplied with the sheets by the Dow Chemical Company indicate strong basal plane textures, with a slightly greater spread toward the rolling direction than toward the transverse direction. With this texture, slip on either prismatic or pyramidal planes ought to lead to R values higher than those given above. The low experimental values cannot be

explained by $\{10\bar{1}2\}\langle 10\bar{1}1\rangle$ twinning because this should not occur under tension. The only other rationale for these results is that slip occurs on the basal plane despite its unfavorable orientation. The increase of R value with strain may be a consequence of the higher stresses acting to introduce more non-basal slip. Should the explanation be correct, a general increase of R would be expected at higher temperatures since the shear stress for non-basal slip decreases more rapidly with temperature than that for basal slip.

Before the plastic anisotropy of HCP metals can be related quantitatively to crystallographic textures, more information is required about the roles played by the several possible slip and twinning systems in the deformation of polycrystalline material. Deformation experiments on constrained single crystals are planned to generate such information. Several orientations of magnesium crystals are now being grown for plane-strain compression testing, the orientations being selected so that different slip or twinning systems will be activated. The resulting stress-strain curves and metallographic observations should aid materially in determining the relative importance of the different deformation mechanisms in textured polycrystals.

Theoretical Analysis of Plastic Anisotropy in Cubic Metals

In cubic metals, slip is by far the most important deformation mechanism. Except for low temperature twinning and high-temperature grain boundary sliding, it accounts for virtually all plastic flow. The FCC metals have four $\{111\}$ slip planes each containing three $\langle 110\rangle$ slip directions, making a total of 12 possible $\{111\}\langle 110\rangle$ slip systems. In the BCC metals, slip

on several types of planes, {110}, {112} and {123}, has been reported, always in one of the four ⟨111⟩ directions.

With their greater multiplicity of slip systems, BCC and FCC metals are somewhat less anisotropic than HCP metals, and the reason for the anisotropy is not as obvious. However, a method for predicting quantitatively the effects of crystallographic texture on plastic properties of FCC metals has been devised. It also applies to BCC metals deforming by $\{110\}\langle 111\rangle$ slip. This method is an extension of the analysis that Taylor developed for calculating the tensile (or compressive) stress-strain curves of randomly oriented polycrystals from the stress-strain curves of single crystals. Before presenting the new method, it is useful to review the Taylor analysis.[2,3,4]

The Taylor Analysis: This is based on determining the amount of slip required in each grain during deformation, relating the strength of the grain to that amount of slip, and finding the average strength of grains with all possible orientation. When a polycrystalline metal is deformed, each grain changes shape in such a way as to maintain contact with neighboring grains. To account for continuity of displacements at grain boundaries, it was assumed that every grain undergoes the same strain as the aggregate in which it is imbedded. Under tensile loading the flow of a randomly oriented polycrystal is axially symmetric, the strains of the aggregate and therefore of the individual grains being:

$$\epsilon_y = \epsilon_z = -1/2\ \epsilon_x;\ \epsilon_{yz} = \epsilon_{zx} = \epsilon_{xy} = 0 \qquad (3)$$

where x, y and z are orthogonal axes, x being the axis of stressing. The single subscripts indicate normal strain and the double subscripts indicate shear strains, i.e., ϵ_x is the tensile strain parallel to x and ϵ_{xy} is the shear strain in the x plane and y direction.

To avoid later complications introduced by the rotation of crystal axes during deformation, attention will be focused here on the relations between small or incremental strains. For incremental strains, Eq. 3 becomes

$$d\epsilon_y = d\epsilon_z = -1/2\ d\epsilon_x; \quad d\epsilon_{yz} = d\epsilon_{zx} = d\epsilon_{xy} = 0. \tag{4}$$

For a grain with a given crystallographic orientation, the set of strain increments relative to the specimen axes may be transformed into an equivalent set, $d\epsilon_1$, $d\epsilon_2$, $d\epsilon_3$, $d\epsilon_{23}$, $d\epsilon_{31}$, $d\epsilon_{12}$, relative to the cube axis of the grain. With constant volume,

$$d\epsilon_1 + d\epsilon_2 + d\epsilon_3 = 0 \tag{5}$$

or

$$d\epsilon_3 = -(d\epsilon_1 + d\epsilon_2),$$

and the number of independent strains is five. To produce these strains, five or more of the twelve slip systems must be operative. Not every combination of five slip systems can be used, however. To produce an arbitrary shape change, the five slip systems must be independent in the sense that the

shear caused by one could not be produced by any combination of the others. To identify the operative systems, Taylor assumed that only those would be active which gave the minimum value of $M = d\gamma/d\epsilon_x$, where $d\gamma$ is the sum of the incremental shear strains on all of the active slip systems needed to produce an increment of tensile strain, $d\epsilon_x$. The minimum M value appropriate for a given orientation was obtained after first calculating values for many possible possible combinations of slip systems. Such calculations were made for grains of each of a number of orientations in the basic stereographic triangle, and the average value was found to be $\overline{M} = 3.06$.*

The next step was to relate the stress, σ_x, required for a grain to flow with axial symmetry to the total shear strain increment, $d\gamma$. This was accomplished by assuming further that the shear stress, τ, to active slip would be the same for all systems, the work expended in slip throughout a unit volume of material then becoming

$$dW = \tau d\gamma \tag{6}$$

which must be identical to the work per unit volume done by the applied stress in producing the extension

$$dW = \sigma_x \, d\epsilon_x \, . \tag{7}$$

---

* In Taylor's original work, many possible combinations of slip systems were still overlooked. However, the same $\overline{M} = 3.06$ was later found by Bishop and Hill in an independent and more thorough analysis.[5]

Equating (6) and (7),

$$\frac{\sigma_x}{\tau} = \frac{d\gamma}{d\epsilon_x} = M = \frac{dW}{\tau d\epsilon_x} . \qquad (8)\star$$

In addition to relating the incremental shear and axial strains, M serves also to relate the tensile flow σ_x of a grain to the basic shear stress τ for slip. Thus M is, in effect, a relative strength.

Finally, the tensile stress-strain or $\sigma_x - \epsilon_x$ curve for a randomly oriented polycrystal was obtained from the $\tau - \gamma$ curve for a single crystal of the same material by using the $\bar{M}$ averaged over all orientations ($\bar{M} = 3.06$) and by neglecting changes in $\bar{M}$ from lattice rotation. Points on the $\sigma_x - \epsilon_x$ curve at $\sigma_x = 3.06\tau$ and $\epsilon_x = \frac{\gamma}{3.06}$ were simply taken from the corresponding points on the $\tau - \gamma$ curve. The polycrystalline $\sigma - \epsilon$ curve constructed in this way for aluminum was in reasonable agreement with experiment.

---

* Equation 8 is the multiple slip analog of the Schmid law[6] for single slip:

$$\frac{\sigma_x}{\tau} = \frac{d\gamma}{d\epsilon_x} = \frac{1}{\cos\lambda \cos\phi}$$

where λ and ϕ are the angles between x and the slip direction and the slip-plane normal, respectively.

An Analysis by Bishop and Hill: More recently an equivalent but simpler method has been devised for calculating M in grains of various orientations.[5,7] Simultaneous slip on five or more systems can occur only when the critical stress for slip, τ, is reached on these systems without being exceeded on any others. Bishop and Hill showed that this condition is satisfied only with a limited number of stress states or combinations of the terms, $A = \frac{\sqrt{6}}{\tau}(\sigma_2 - \sigma_3)$, $B = \frac{\sqrt{6}}{\tau}(\sigma_3 - \sigma_1)$, $C \frac{\sqrt{6}}{\tau}(\sigma_1 - \sigma_2)$, $F = \frac{\sqrt{6}}{\tau}\sigma_{23}$, $G = \frac{\sqrt{6}}{\tau}\sigma_{31}$, and $H = \frac{\sqrt{6}}{\tau}\sigma_{12}$, where the stresses σ are taken with reference to the cube axes of the crystal. The actual values that these terms may assume turn out to be 0, $\pm$ 1/2, $\pm$ 1.

An expanded form of Eq. 8 is useful for calculating M.

$$M = \frac{dw}{\tau d\epsilon_x} = \frac{1}{\tau}\left[\sigma_1 \frac{d\epsilon_1}{d\epsilon_x} + \sigma_2 \frac{d\epsilon_2}{d\epsilon_x} \sigma_3 \frac{d\epsilon_3}{d\epsilon_x} + 2\,\sigma_{23} \frac{d\epsilon_{23}}{d\epsilon_x} + 2\,\sigma_{31}\frac{d\epsilon_{31}}{d\epsilon_x} + 2\,\sigma_{12} \frac{d\epsilon_{12}}{d\epsilon_x}\right] \tag{9}$$

Substituting the constant-volume relationship, Eq. 5,

$$M = \frac{1}{\tau}\left[(\sigma_1 - \sigma_3) \frac{d\epsilon_1}{d\epsilon_x} + (\sigma_2 - \sigma_3) \frac{d\epsilon_2}{d\epsilon_x} + 2\,\sigma_{23} \frac{d\epsilon_{23}}{d\epsilon_x} + 2\,\sigma_{31} \frac{d\epsilon_{31}}{d\epsilon_x} + 2\,\sigma_{12} \frac{d\epsilon_{12}}{d\epsilon_x}\right] \tag{10}$$

or

$$M = \sqrt{6}\left[-B\frac{d\epsilon_1}{d\epsilon_x} + A\frac{d\epsilon_2}{d\epsilon_x} + 2F\frac{d\epsilon_{23}}{d\epsilon_x} + 2G\frac{d\epsilon_{31}}{d\epsilon_x} + 2H\frac{d\epsilon_{12}}{d\epsilon_x}\right]. \qquad (11)$$

M is evaluated for a given orientation (of cube axis relative to specimen axes) and for a specified shape change, defined by the ratios of the strain components along the specimen axes. The essential steps are outlined below:

1. The strain components along the specimen axes, x, y and z, are resolved into components along the cube axes of the crystal, 1, 2 and 3, with the expression, for $d\epsilon_1$,

$$d\epsilon_1 = \ell_{1x}^2\, d\epsilon_x + \ell_{1y}^2\, d\epsilon_y + \ell_{1z}^2\, d\epsilon_z + \ell_{1y}\ell_{1z}\, d\epsilon_{yz} + \ell_{1z}\ell_{1x}\, d\epsilon_{zx} + \ell_{1x}\ell_{1y}\, d\epsilon_{xy}$$

and similar fomulations for the other normal and shear-strain components; the ℓ terms are the cosines of the angles between cube axes and the specimen axes.

2. If a relationship between $d\epsilon_x$, $d\epsilon_y$, $d\epsilon_z$, $d\epsilon_{zx}$, and $d\epsilon_{xy}$ is known, the strains along the cube axes are found relative to $d\epsilon_x$ and substituted into Eq. 11. For example, if the flow is axially symmetric (Eq. 4),

$$\frac{d\epsilon_1}{d\epsilon_x} = \ell_{1x}^2 - 1/2\,\ell_{1y}^2 - 1/2\,\ell_{1z}^2, \text{ etc.}$$

3. Finally, Eq. 11 is evaluated for each possible combination of A, B, ... H. The largest result is selected as the appropriate M value according to the principal of maximum virtual work.

Strength of Fiber Texture: Equation 11 was used to establish the orientation dependence of M for axially symmetric flow over the full stereographic triangle (Fig. 2). An average value of M,° identifying the relative strength of a randomly oriented polycrystal, has been calculated on this basis. However, the results may also be applied directly to predict the relative strength of wires with different fiber textures which also extend in axially symmetric flow. The strength is indicated by the M value corresponding to the orientation of the fiber axis. Thus a wire with a [111] or [110] fiber texture should be 50% stronger than one with a [100] texture and about 20% stronger than if it were randomly oriented. The same relative strengths would be expected in compression.

Yielding and Plastic Strain in Textured Sheets: It was shown in the previous report that when texture-hardening was introduced, the yielding of a sheet being compressed in the thickness direction is equivalent to yielding under a state of balanced biaxial tension in the plane of the sheet. Accordingly, Fig. 2 may also be used to predict yielding resistance under the latter condition of loading if the texture is rotationally symmetric about the sheet normal. Therefore, textural components with [111] and [110] normal to the sheet have the effect of increasing strength when loads are applied in this way. As noted before, the same texture would also strengthen a sheet even if the principal tensile stresses should be somewhat "unbalanced".

The analysis may be broadened to include the anisotropy of yielding in textured sheets under simple tension. Of interest here are both the tensile yield stress and the width-to-thickness strain ratio $R = \frac{d\epsilon_y}{d\epsilon_z}$ of specimens taken in different directions in the sheet. To apply the analysis, the incremental shear-strain $d\gamma$ corresponding to $d\epsilon_x$ must be found, but this can be calculated only after the other normal strain increments are known relative to $d\epsilon_x$. If the tensile axis, x, is taken parallel to one of the principal axes of anisotropy, it is still reasonable to assume $d\epsilon_{yz} = d\epsilon_{zx} = d\epsilon_{xy} = 0$. Constancy of volume (Eq. 5) applies. Yet one strain component, $d\epsilon_y$ or $d\epsilon_z$, remains unspecified; this may be incorporated in a useful parameter

$$r = \frac{d\epsilon_y}{d\epsilon_y + d\epsilon_z} = \frac{R}{R + 1} , \tag{12}$$

so that

$$d\epsilon_y = - r\, d\epsilon_x ; \quad d\epsilon_z = - (1 - r)\, d\epsilon_x .$$

Now the ratios,

$$\frac{d\epsilon_1}{d\epsilon_x}, \frac{d\epsilon_2}{d\epsilon_x}, \frac{d\epsilon_{23}}{d\epsilon_x}, \frac{d\epsilon_{31}}{d\epsilon_x} \text{ and } \frac{d\epsilon_{12}}{d\epsilon_x}$$

in Eq. 11 can be expressed in terms of r, as

$$\frac{d\epsilon_1}{d\epsilon_x} = \ell_{1x}^2 - r\, \ell_{1y}^2 - (1 - r)\ell_{1z}^2 , \text{ etc.}$$

By assuming different values of r and calculating the corresponding values of $M = \frac{d\gamma}{d\epsilon_x}$ from Eq. 11, an M vs. r plot may be generated. The minimum M of such a plot represents the least slip or least work with which the strain increment $d\epsilon_x$ could be produced and therefore corresponds to the expected behavior. The values of M and r at the minimum identify the relative strength $\frac{\sigma_x}{\tau}$ and the strain ratio $R = \frac{r}{1 - r}$.

As an example, consider tension tests made on a sheet with the ideal $[1\bar{1}2]$ (110) texture characteristic of cold-rolled alpha-brass,[8] (Fig. 3). From the minimum M of the M vs. r curve for a rolling-direction test, values R = 1 and $\frac{\sigma_x}{\tau} = 3.10$ are predicted. For a transverse direction test, the flat minimum from r = 0.125 to r = 1.0 makes the prediction of a single R impossible. In these plots each straight line section corresponds to the combination of A, B, F, G, and H which maximizes M in Eq. 11. For a sheet with an ideal $[1\bar{1}0]$ (111) (a textural component of cold-rolled steel[8]) tested in the rolling direction, the M vs. r curve is a single straight line sloping downward with increasing r so that an infinite R is predicted (Fig. 4). While these predictions are made for single ideal textures, small amounts of other textural components would modify the results, probably creating a unique minimum for the $[1\bar{1}2]$ (110) transverse test (Fig. 3) and shifting the minimum to finite R values in the $[1\bar{1}0]$ (111) rolling-direction test (Fig. 4).

The value of such calculations for ideal textures lies in the way results may be combined to predict the behavior of textured sheets of mixed components. The M vs. r curve for a material consisting of several textural components a, b, ... may be found from the weighted average

$$M = f_a M_a + f_b M_b \cdots , \qquad (13)$$

where f_a and f_b are the volume fractions of components a, b, ... The minimum will occur when

$$\frac{dM}{dr} = f_a \frac{dM_a}{dr} + f_b \frac{dM_b}{dr} + \ldots = 0 \ . \tag{14}$$

If a fraction of the grains is randomly oriented, it can be treated as a component with isotropic plastic properties. The characteristic M vs. r curve for randomly oriented grain may be found by using the von Mises yield criterion and its associated flow rule. With these it can be shown that under an imposed ratio of strain $r = \dfrac{d\epsilon_y}{d\epsilon_y + d\epsilon_z}$ the work per unit volume dW, per increment of strain $d\epsilon_x$ is

$$\frac{dW}{d\epsilon_x} = X \sqrt{4/3 \ (r^2 - r + 1)} \ , \tag{15}$$

where X is the yield stress under uniaxial tension. Combining Eqs. 15 and 8,

$$M = \frac{X}{\tau} \sqrt{4/3 \ (r^2 - r + 1)} \ . \tag{16}$$

Using Taylor's value for the tensile yield stress of a randomly oriented polycrystal, $\frac{X}{\tau} = \bar{M} = 3.06$. Therefore

$$M = 3.06 \sqrt{4/3 \ (r^2 - r + 1)} \tag{17}$$

describes the shape of the M vs. r curve for randomly oriented grains (Fig. 4). Because of the shape of this curve, the presence of some randomly oriented grains in a textured sheet will make R move toward unity. For example in a sheet with the $[1\bar{1}0]$ (111) texture, if half of the grains become randomly oriented the minimum occurs at R = 2.33 instead of at R = ∞ (Fig. 4).

The present analysis may be used to predict R values for sheets with textures that are rotationally symmetric about the sheet normal. With a crystallographic plane, (hkl) parallel to the rolling plane, all directions in (hkl) will be aligned with the axis of a tensile specimen cut from the sheet. For the purpose of analysis, such a texture has been approximated with a number of components, each sharing the common (hkl) plane, but differing from one another by 5° or 10° rotations about the normal to the sheet. Figures 5, 6, and 7 show the M vs. r curves for each of the various components of the textures with (100), (110) and (111) respectively in the plane of the sheet. By averaging the curves for the various components, M vs. r curves were obtained for rotationally symmetric textures with (100), (110) and (111) planes in the sheet (Fig. 8). Although pure (111) and (110) textures should give infinite R values, a small amount of some other component would preclude this possibility. The curve for randomly oriented grains is added for comparison.

The calculated curves may be related to the observations of Whiteley and Wise[9] on steel sheets. When these authors evaluated the relative amounts of (111), (110) and (100) components and compared the results with experimental R values, they found that (111) contributed to high R, (110) was

neutral, while a small amount of (100) strongly depressed R. Such findings are consistent with the slopes dM/dr of the three curves in the range r = 1/2 to 2/3 (R = 1 to 2) that characterized their steels. If only (111) and (100) were present, the minimum M would occur when $f_{(100)} \frac{dM_{(100)}}{dr} + f_{(111)} \frac{dM_{(111)}}{dr} = 0$. At R = 1.5, $\frac{dM_{(100)}}{dr} = .9$ and $\frac{dM_{(111)}}{dr} = -.2$ so that the effect of a (100) component in depressing R would balance the elevating effect of 4 to 5 times as much (111) component.

Limitation of the Analysis: It is important to consider the limitations involved in extending Taylor's analysis to the prediction of plastic anisotropy in cubic metals. The basic assumptions of the original theory were that deformation is homogeneous (each grain undergoes the same shape change as the polycrystalline aggregate), that the active slip systems are determined by the condition of least shear, and that the work hardening of all active slip systems is the same and depends only on the total amount of prior slip. These assumptions may form the bases for several reasonable objections to the analysis.

Sometimes during deformation the individual grains of a polycrystal may undergo shape changes which are quite different from those of the polycrystal itself. In [110] fiber-textured wires of iron and tungsten, the grains are ribbon-shaped instead of cigar-shaped after drawing.[10] During the compression of polycrystalline aluminum, the flow of individual grains strongly departs from axial symmetry once a [110] texture is developed.[11] The formation of deformation bands represents still another departure from homogeneous flow. The deviations from assumed behavior which are usually not large, probably

occur in such a way as to lower the total amount of work so that the predicted strengths should be regarded as reasonable upper bounds to actual values.

The assumption that work hardening depends only on the total amount of prior slip might be questioned in view of the different combinations of slip systems and dislocation interactions that would prevail in differently oriented grains. If this were a major complication, the orientation dependence of strength could not be described by M alone. To test the point, work hardening was recently studied in aluminum crystals subjected to constrained axially-symmetric flow by drawing through dies.[11] The results indicated that the orientation dependence of strength was in fact adequately described by the variation of M over the stereographic triangle.

Applying the analysis to BCC metals involves the assumption that slip is restricted to $\{110\}\langle 111\rangle$ systems. Apparent slip on $\{112\}$, $\{123\}$ and non-crystallographic planes may be due to frequent cross-slip of screw dislocations from one $\{110\}$ plane to another, which should occur readily. Even if slip does occur on other crystallographic planes, the prediction of the analysis still ought to have value for suggesting useful textural components. The reason is that in the analysis, restricting slip to 4 $\langle 111\rangle$ directions is more severe than confining slip to 6 $\{110\}$ planes; and the former restriction accounts for a greater part of the anisotropy.

There seems to be no reasonable way, however, to extend the present analysis to HCP metals, in which the many slip and twinning systems have different critical stresses for operation.

References

1. R. Hill, Mathematical Theory of Plasticity, Oxford Univ. Press, London, 1950, 315; Proc. Roy. Soc. (London), A, 193 (1948) 281.

2. G. I. Taylor, J. Inst. Metals, 62 (1938) 307.

3. G. I. Taylor, in Stephen Timoshenko Anniversary Volume, Macmillan Co., New York, 1938, 218.

4. G. I. Taylor, in Colloquium Madrid: Deformation and Flow of Solids, Springer-Verlag, Berlin, 1956, 3.

5. J. F. W. Bishop and R. Hill, Phil. Mag., 42 (1951) 414 and 1298.

6. E. Schmid and W. Boas, Plasticity of Crystals, F. A. Hughes and Co.

7. J. F. W. Bishop, Phil. Mag., 44 (1953) 51.

8. C. S. Barrett, Structure of Metals, McGraw-Hill Book Co., New York, 1952.

9. R. L. Whiteley and D. E. Wise, paper presented at Fourth Mechanical Working Conference; Flat Rolled Products, AIME Chicago, 1962.

10. J. F. Peck and D. A. Thomas, Trans. AIME, 221 (1961) 1240.

11. W. F. Hosford, Jr., to be published.

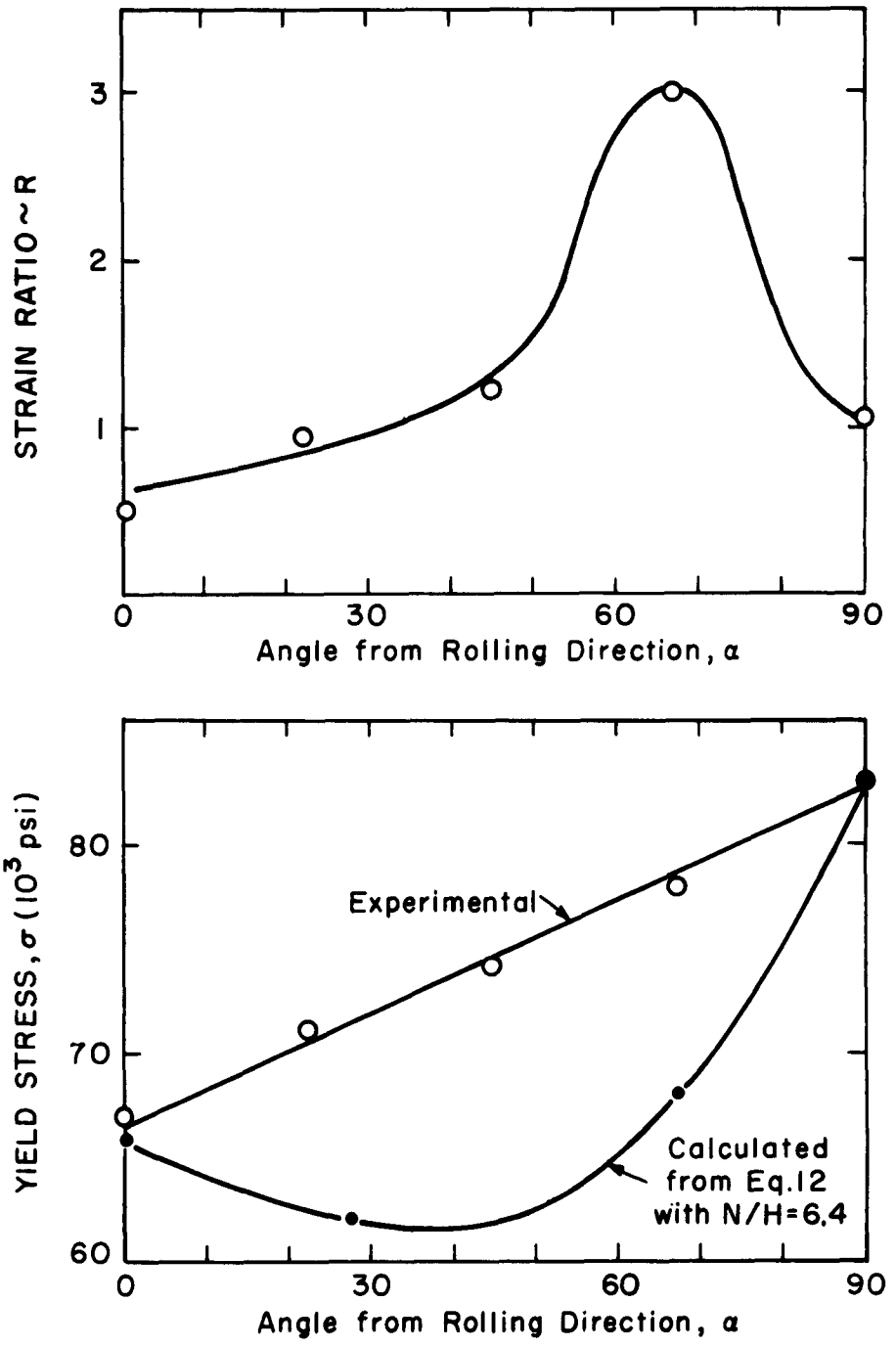

Fig. 1. Angular dependence of strain ratio, R, and tensile yield stress, σ, in strip tensile specimens cut from a titanium sheet (RC-70, annealed).

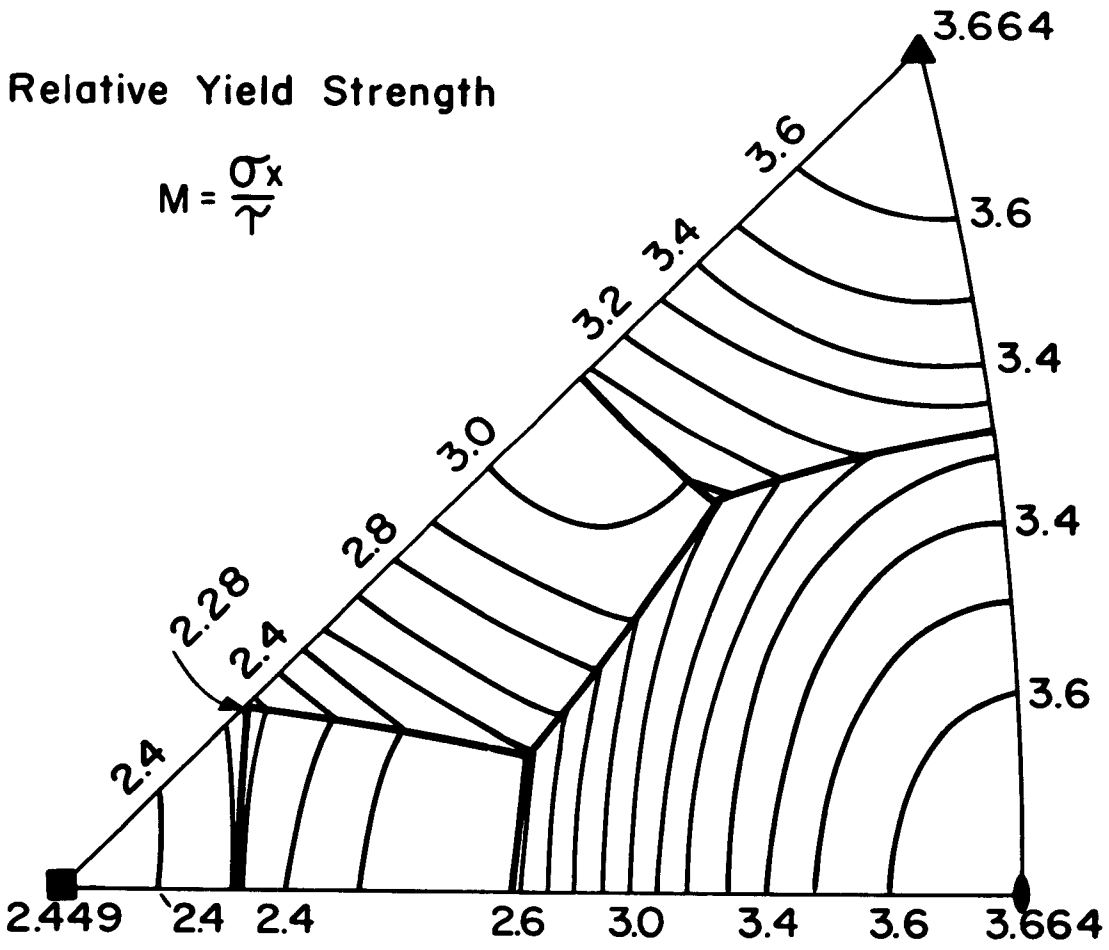

Fig. 2. Orientation dependence of M for axially symmetric flow.

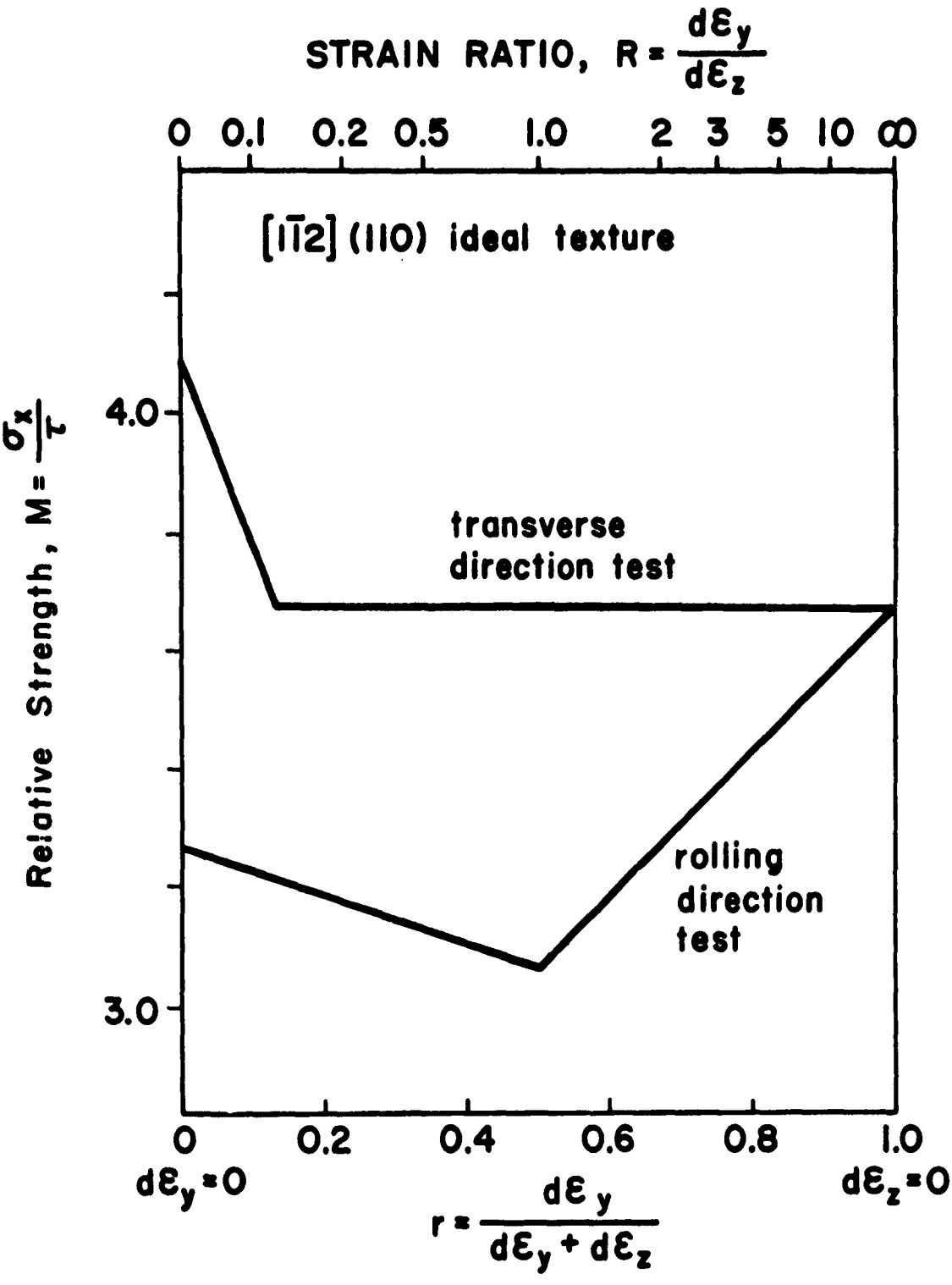

Fig. 3. Dependence of M on r for rolling and transverse direction tension tests in a sheet of ideal [1T2] (110) texture. Expected behavior corresponds to lowest M values.

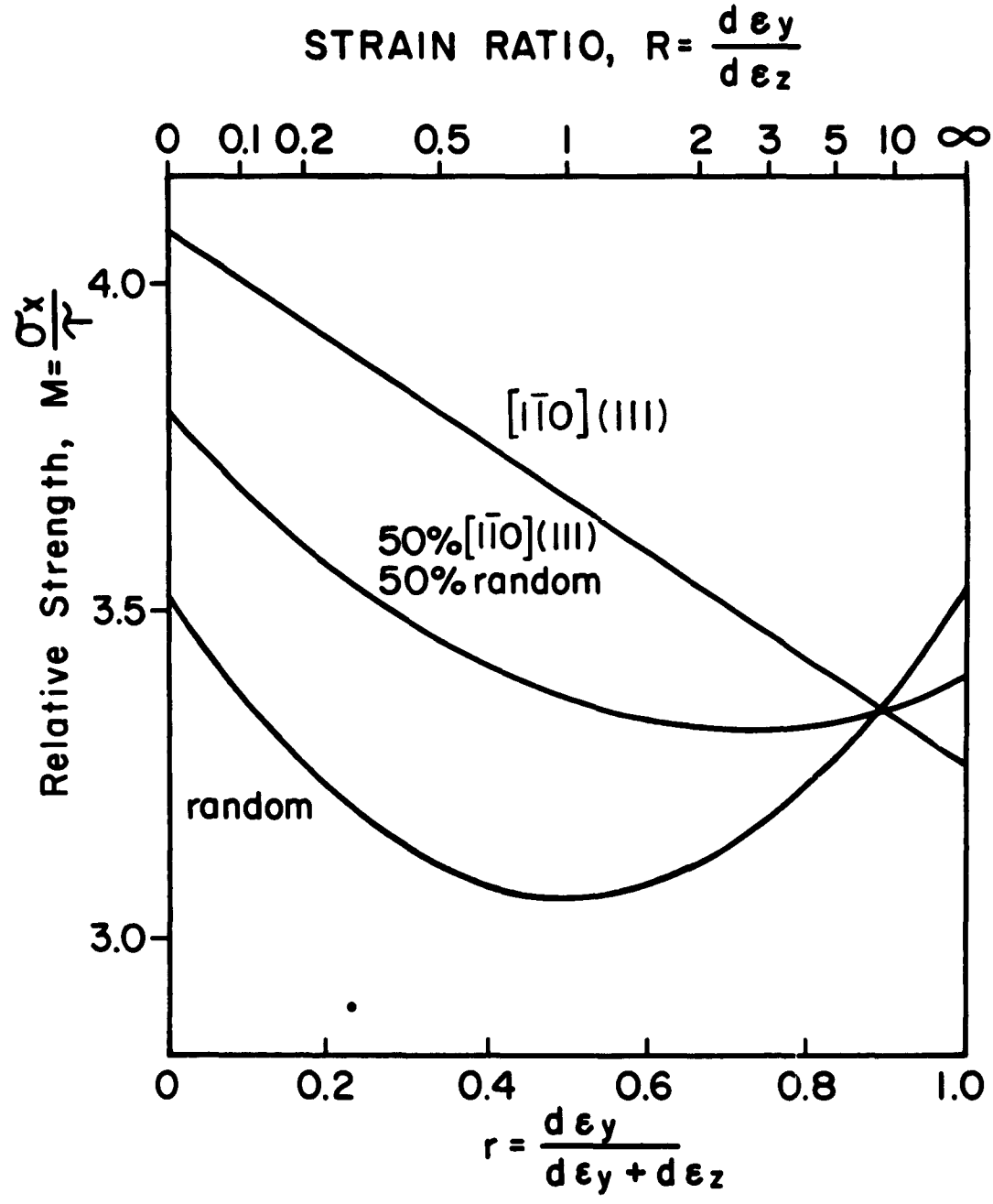

Fig. 4. Dependence of M on r for rolling direction tension tests of sheets with ideal [1T0] (111) texture, with randomly oriented grains, and with equal mixture of ideal [1T0] (111) and random components. The presence of 50% randomly oriented grains shifts the minimum M from r = 1, (R = ∞) to r = 0.7, (R = 2.33).

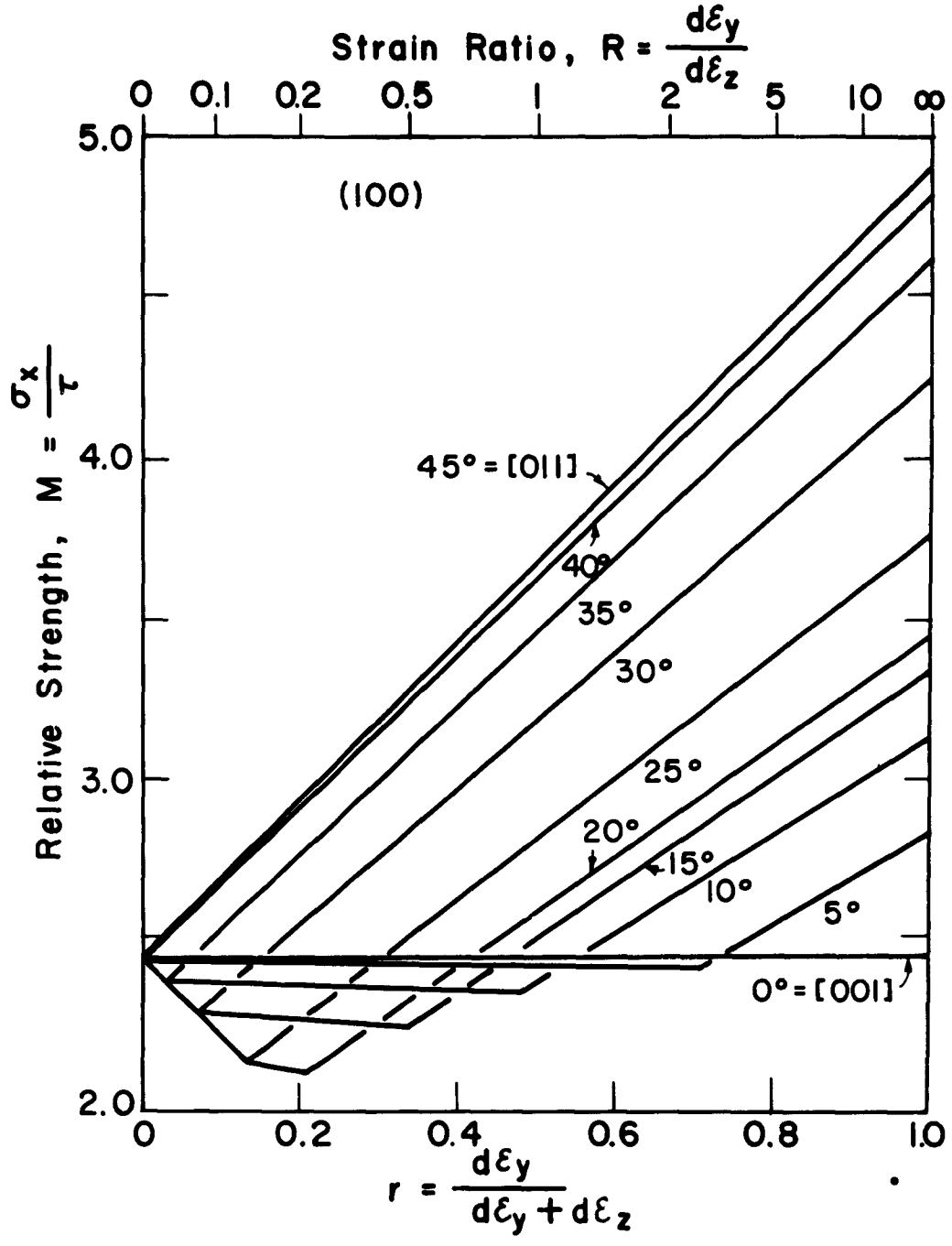

Fig. 5. M vs. r curves for various components of a (100) sheet texture. Angles between tensile axis and [001] are indicated for each component.

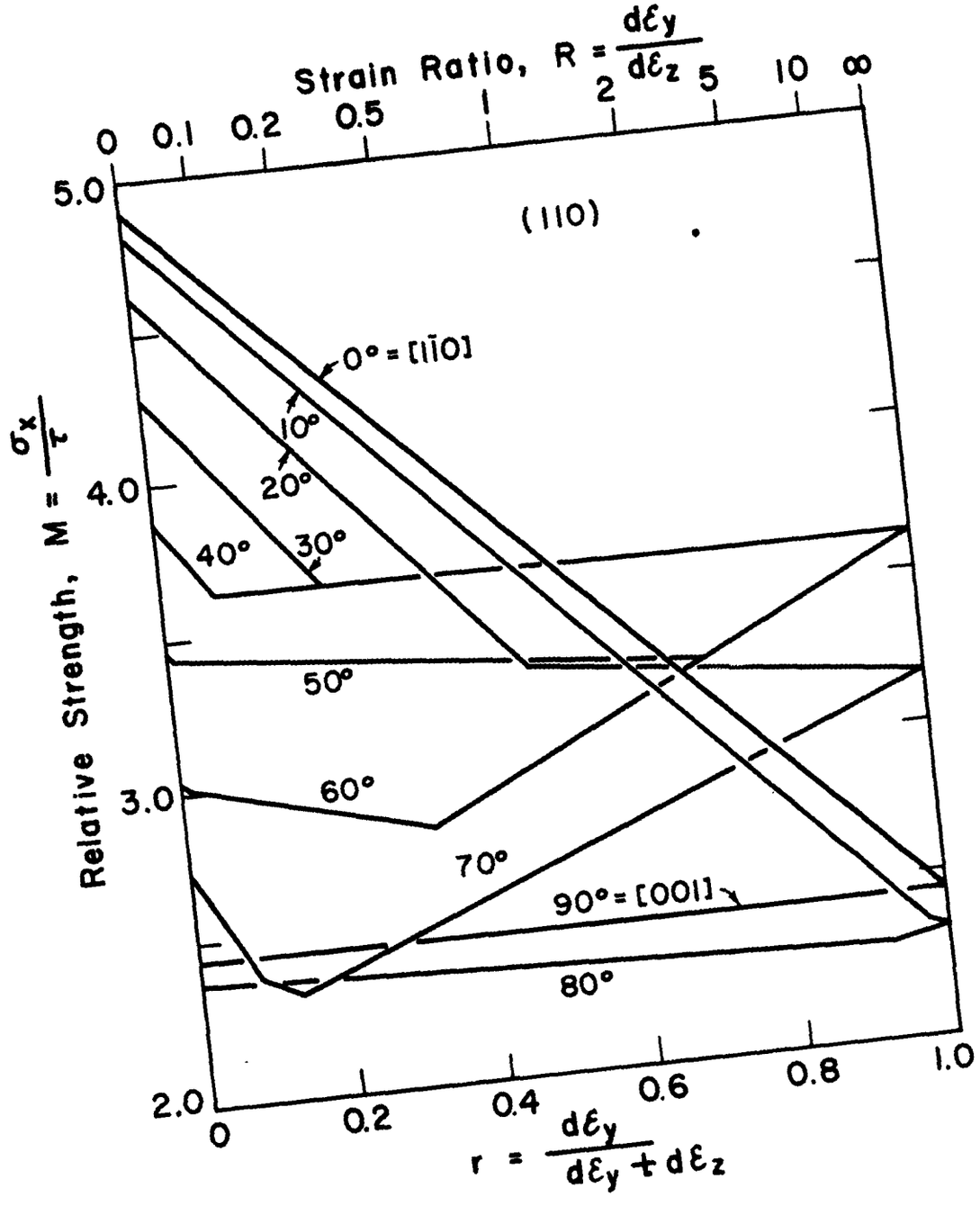

Fig. 6. M vs. r curves for various components of a (110) sheet texture. Angles between tensile axis and [1$\bar{1}$0] are indicated for each component.

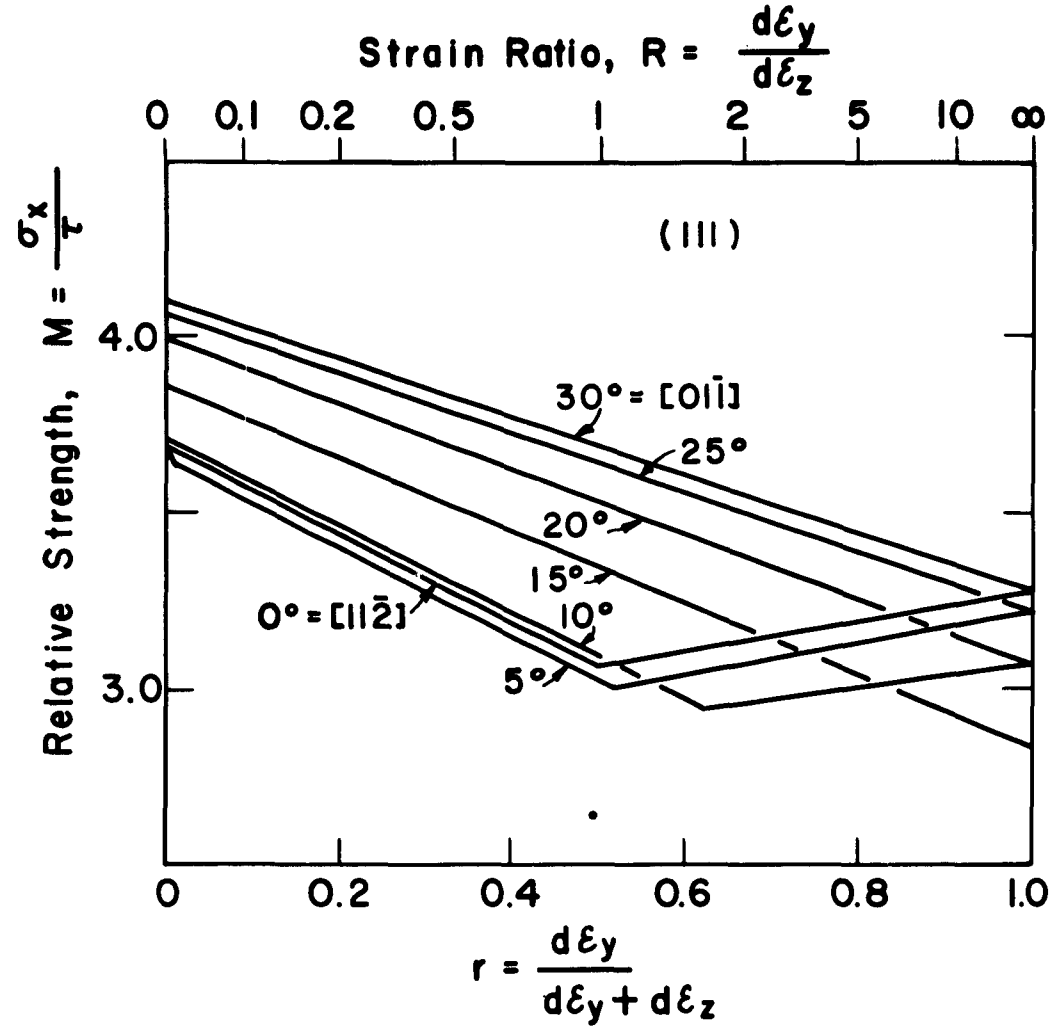

Fig. 7. M vs. r curves for various components of a (111) sheet texture. Angles between tensile axis and $[11\bar{2}]$ are indicated for each component.

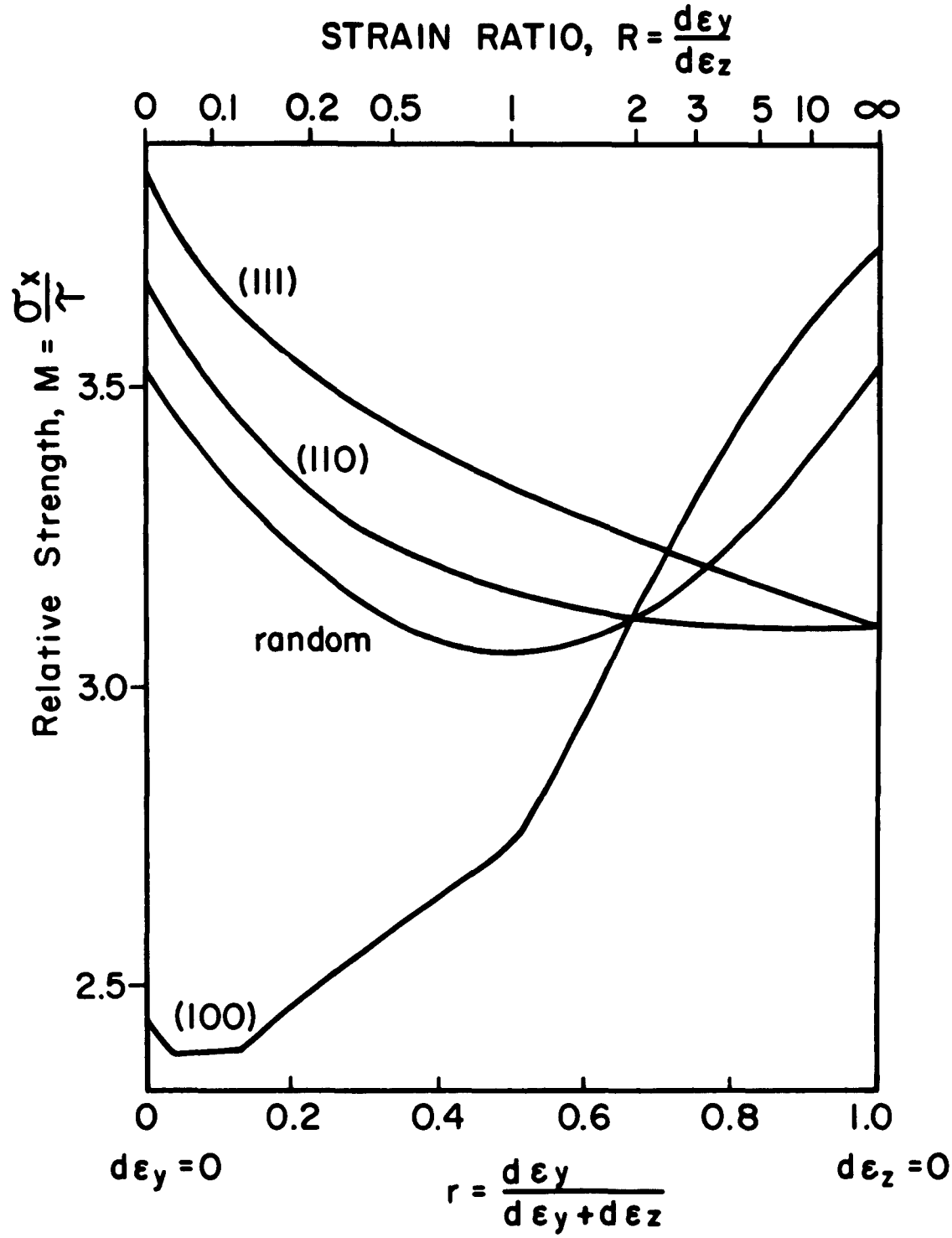

Fig. 8. M vs. r curves for textures which are rotationally symmetric about the sheet normal. Curves are shown for sheets in which (111), (110) and (100) are parallel to the rolling plane, and for randomly oriented sheets.

AD_____ and Accession No._____
Massachusetts Institute of Technology, Cambridge, Mass.
STRENGTH AND PLASTICITY OF ANISOTORPIC METALS;
SECOND QUARTERLY REPORT.
W.A. Backofen, W.F. Hosford, Jr., M.I.T., Cambridge, Massachusetts.

Report No. WAL TR 834.12/2-1, December 1962,
26 pages, (Contract No. DA-19-020-ORD-5719)
DA Project 59332008, Unclassified Report

The angular variations of tensile yield stress and strain ratio measured in a sheet of RC-70 titanium are not consistent with the predictions of Hill's anisotropic plasticity theory. Relatively low R values are reported for AZ 31B magnesium alloy sheets, despite strong (0001) textures.

A method is outlined for calculating the relationship of plastic anisotropy to crystallographic texture for cubic metals. Predictions are made of the texture dependence of flow stress and strain ratio.

NO DISTRIBUTION LIMITATIONS

Unclassified

1. Plastic deformation
2. Plasticity
3. Stress and strain
4. Contract DA-19-020-ORD-5719

Massachusetts Institute of Technology.

AD_____ and Accession No._____
Massachusetts Institute of Technology, Cambridge, Mass.
STRENGTH AND PLASTICITY OF ANISOTORPIC METALS;
SECOND QUARTERLY REPORT.
W.A. Backofen, W.F. Hosford, Jr., M.I.T., Cambridge, Massachusetts.

Report No. WAL TR 834.12/2-1, December 1962,
26 pages, (Contract No. DA-19-020-ORD-5719)
DA Project 59332008, Unclassified Report

The angular variations of tensile yield stress and strain ratio measured in a sheet of RC-70 titanium are not consistent with the predictions of Hill's anisotropic plasticity theory. Relatively low R values are reported for AZ 31B magnesium alloy sheets, despite strong (0001) textures.

A method is outlined for calculating the relationship of plastic anisotropy to crystallographic texture for cubic metals. Predictions are made of the texture dependence of flow stress and strain ratio.

NO DISTRIBUTION LIMITATIONS

Unclassified

1. Plastic deformation
2. Plasticity
3. Stress and strain
4. Contract DA-19-020-ORD-5719

Massachusetts Institute of Technology.

AD_____ and Accession No._____
Massachusetts Institute of Technology, Cambridge, Mass.
STRENGTH AND PLASTICITY OF ANISOTORPIC METALS;
SECOND QUARTERLY REPORT.
W.A. Backofen, W.F. Hosford, Jr., M.I.T., Cambridge, Massachusetts.

Report No. WAL TR 834.12/2-1, December 1962,
26 pages, (Contract No. DA-19-020-ORD-5719)
DA Project 59332008, Unclassified Report

The angular variations of tensile yield stress and strain ratio measured in a sheet of RC-70 titanium are not consistent with the predictions of Hill's anisotropic plasticity theory. Relatively low R values are reported for AZ 31B magnesium alloy sheets, despite strong (0001) textures.

A method is outlined for calculating the relationship of plastic anisotropy to crystallographic texture for cubic metals. Predictions are made of the texture dependence of flow stress and strain ratio.

NO DISTRIBUTION LIMITATIONS

Unclassified

1. Plastic deformation
2. Plasticity
3. Stress and strain
4. Contract DA-19-020-ORD-5719

Massachusetts Institute of Technology.

AD_____ and Accession No._____
Massachusetts Institute of Technology, Cambridge, Mass.
STRENGTH AND PLASTICITY OF ANISOTORPIC METALS;
SECOND QUARTERLY REPORT.
W.A. Backofen, W.F. Hosford, Jr., M.I.T., Cambridge, Massachusetts.

Report No. WAL TR 834.12/2-1, December 1962,
26 pages, (Contract No. DA-19-020-ORD-5719)
DA Project 59332008, Unclassified Report

The angular variations of tensile yield stress and strain ratio measured in a sheet of RC-70 titanium are not consistent with the predictions of Hill's anisotropic plasticity theory. Relatively low R values are reported for AZ 31B magnesium alloy sheets, despite strong (0001) textures.

A method is outlined for calculating the relationship of plastic anisotropy to crystallographic texture for cubic metals. Predictions are made of the texture dependence of flow stress and strain ratio.

NO DISTRIBUTION LIMITATIONS

Unclassified

1. Plastic deformation
2. Plasticity
3. Stress and strain
4. Contract DA-19-020-ORD-5719

Massachusetts Institute of Technology.

Massachusetts Institute of Technology
Contract No. DA-19-020-ORD-5719
WAT-2690

DISTRIBUTION LIST

	No. of Copies
A. Department of Defense	
Office of the Director of Defense Research & Engineering ATTN: Mr. J. C. Barrett Room 3D-1067, The Pentagon Washington 25, D. C.	1
Armed Services Technical Information Agency ATTN: TIPDR Arlington Hall Station Arlington 12, Virginia	10
Defense Metals Information Center Battelle Memorial Institute Columbus, Ohio	1
Solid Propellant Information Agency Applied Physics Laboratory The Johns Hopkins University Silver Spring, Maryland	3
B. Department of the Army - Technical Services	
Office Chief of Ordnance ATTN: ORDTB-Materials Department of the Army Washington 25, D. C.	1
Commanding General Aberdeen Proving Ground ATTN: Dr. C. Pickett, C&CL Aberdeen Proving Ground, Maryland	1
Commanding General Ordnance Tank-Automotive Command ATTN: Mr. S. Sobak, ORDMC-IF-2 Detroit 9, Michigan	1
Commanding General Ordnance Weapons Command ATTN: Mr. B. Gerke, ORDOW-IA Rock Island, Illinois	1

DISTRIBUTION LIST

	No. of Copies
Commanding General U.S. Army Ordnance Missile Command	
ATTN: Documentation & Technical Information Branch	2
Mr. R. E. Ely, ORDXM-RRS	1
Mr. R. Fink, ORDXM-RKX	1
Mr. W. K. Thomas, ORDXM	1
Mr. E. J. Wheelahan, ORDXM-RSM	1
Redstone Arsenal, Alabama	
Commanding General U.S. Army Ordnance Special Weapons Ammunition Command Dover, New Jersey	1
Commanding Officer Diamond Ordnance Fuze Laboratory ATTN: Technical Library Washington 25, D. C.	4
Commanding Officer Frankford Arsenal	
ATTN: Dr. H. Gisser, ORDBA-1330	1
Mr. H. Markus, ORDBA-1320	1
Mr. E. Roffman, ORDBA-1740	1
Philadelphia 37, Pa.	
Commanding Officer Ordnance Materials Research Office Watertown Arsenal ATTN: RPD Watertown 72, Mass.	1
Commanding Officer Picatinny Arsenal	
ATTN: Mr. J. J. Scavuzzo, Plastics & Packaging Lab.	3
Mr. D. Stein, ORDBB-DE3	1
Dover, New Jersey	
Commanding Officer PLASTEC Picatinny Arsenal Dover, New Jersey	1
Commanding Officer Rock Island Arsenal ATTN: Materials Section, Laboratory Rock Island, Illinois	1

DISTRIBUTION LIST

	No. of Copies
Commanding Officer Springfield Armory ATTN: Mr. R. Korytoski, Research Materials Lab. Springfield 1, Mass.	1
Commanding Officer Watertown Arsenal ATTN: ORDBE-LX Watertown 72, Mass.	3
Commanding Officer Watervliet Arsenal ATTN: Mr. F. Dashnaw, ORDBF-R Watervliet, New York	1
Headquarters U. S. Army Signal R&D Laboratory ATTN: Mr. H. H. Kedesky, SIGRA/SL-XE Fort Monmouth, N. J.	1
Department of the Army - Other Army Agencies	
Commander Army Research Office Office Chief Research & Development ATTN: Physical Sciences Division Pentagon Washington 25, D. C.	2
C. Department of the Navy	
Chief, Bureau of Naval Weapons Department of the Navy ATTN: RMMP Room 2225, Munitions Building Washington 25, D. C.	1
Department of the Navy Office of Naval Research ATTN: Code 423 Washington 25, D. C.	1
Department of the Navy Special Projects Office ATTN: SP 271 Washington 25, D. C.	1

DISTRIBUTION LIST

	No. of Copies
Commander U.S. Naval Ordnance Laboratory ATTN: Code WM White Oak, Silver Spring, Maryland	1
Commander U.S. Naval Ordnance Test Station ATTN: Technical Library Branch China Lake, California	1
Commander U.S. Naval Research Laboratory ATTN: Mr. J. E. Srawley Anacostia Station Washington 25, D. C.	1
D. Department of the Air Force	
U.S. Air Force Directorate of Research & Development ATTN: Lt. Col. J. B. Shipp, Jr. Room 4D-313, The Pentagon Washington 25, D. C.	1
Wright Air Development Division ATTN: H. Zoeller, ASRCEE-1-2 R. F. Klinger, ASRCEM-1 Wright-Patterson Air Force Base, Ohio	2 2
ARDC Flight Test Center ATTN: Solid Systems Division FTRSC Edwards Air Force Base, California	1
AMC Aeronautical Systems Center ATTN: Manufacturing & Materials Technology Div., LMBMO Wright-Patterson Air Force Base, Ohio	2
E. Other Government Agencies	
U.S. Atomic Energy Commission Office of Technical Information Extension P.O. Box 62 Oak Ridge, Tennessee	1
National Aeronautics and Space Administration ATTN: Mr. B. G. Achhammer Mr. G. C. Deutsch Mr. R. V. Rhode Washington, D. C.	1 1 1

DISTRIBUTION LIST

	No. of Copies
Dr. W. Lucas George C. Marshall Space Flight Center, M-S&M-M Huntsville, Alabama	1
Mr. William A. Wilson George C. Marshall Space Flight Center, M-ME-M Huntsville, Alabama	1
Dr. L. Jaffe Jet Propulsion Laboratory California Institute of Technology 4800 Oak Grove Drive Pasadena, California	1
F. Defense Contractors	
Aerojet-General Corporation ATTN: Librarian Post Office Box 1168 Sacramento, California	1
Aerojet-General Corporation ATTN: Librarian Mr. C. A. Fournier Post Office Box 296 Azusa, California	1 1
Allison Division General Motors Corporation ATTN: Mr. D. K. Hanink Indianapolis 6, Indiana	1
ARDE-Portland, Inc. ATTN: Mr. R. Alper 100 Century Road Paramus, N. J.	1
Atlantic Research Corporation ATTN: Mr. E. A. Olcott Shirley Highway and Edsall Road Alexandria, Virginia	1
Curtiss-Wright Corporation Wright Aeronautical Division ATTN: Mr. R. S. Shuris Mr. A. M. Kettle, Technical Library Wood-Ridge, N. J.	1 1

DISTRIBUTION LIST

	No. of Copies
Hercules Powder Company Allegheny Ballistics Laboratory ATTN: Dr. R. Steinberger Post Office Box 210 Cumberland, Maryland	1
Hughes Aircraft Company ATTN: Librarian Culver City, California	1
Rohm & Haas Company Redstone Arsenal Division ATTN: Library Redstone Arsenal, Alabama	1
Tapco Group ATTN: Mr. W. J. Piper 23555 Euclid Avenue Cleveland 17, Ohio	1
Thickol Chemical Corp. Redstone Division ATTN: Library Redstone Arsenal, Alabama	1

SUPPLEMENTAL DISTRIBUTION LIST

	No. of Copies
A. Department of the Navy	
Chief, Bureau of Naval Weapons Department of the Navy ATTN: Mr. P. Goodwin Mr. H. Boertzel Washington 25, D. C.	1 6
Commander U.S. Naval Research Lab. ATTN: Mr. E. Kohn, Code 6110 Anacostia Station Washington 25, D. C.	1
B. Department of the Air Force	
Headquarters Aeronautical Systems Division ATTN: Dr. Tamborski, ASRCNP Wright-Patterson Air Force Base, Ohio	1
Wright Air Development Division ATTN: Mr. G. Peterson, ASRCNC-1 Wright-Patterson Air Force Base, Ohio	1
C. Defense Contractors	
Allegheny Ludlum Steel Corporation Research Center ATTN: Mr. R. A. Lula Brackenridge, Pennsylvania	1
Alloyd Electronics Corporation ATTN: Dr. S. S. White 35 Cambridge Parkway Cambridge, Mass.	1
Aluminum Company of America Alcoa Research Labs. ATTN: Dr. J. L. Brandt Post Office Box 772 New Kensington, Pa.	1
Armco Steel Corporation General Offices ATTN: Mr. J. Barnett Middletown, Ohio	1

SUPPLEMENTAL DISTRIBUTION LIST

	No. of Copies
Battelle Memorial Institute	
ATTN: Mr. R. Monroe	1
Mr. G. Faulkner	1
505 King Avenue	
Columbus 1, Ohio	
The Boeing Company	
Aero Space Division	
P.O. Box 3707	
Seattle 24, Washington	1
Borg-Warner Corporation	
Ingersoll Kalamazoo Division	
ATTN: Mr. L. E. Hershey	
1810 N. Pitcher St.	
Kalamazoo, Michigan	1
The Budd Company	
Defense Division	
ATTN: Mr. R. C. Dethloff	1
Mr. Ohman	1
Philadelphia 32, Pennsylvania	
Climax Molybdenum Company	
ATTN: Mr. R. R. Freeman	
1270 Avenue of the Americas	
New York 20, N. Y.	1
Crucible Steel Co. of America	
ATTN: Mr. W. L. Finlay	
Four Gateway Center	
Pittsburgh 22, Pa.	1
Doublas Aircraft Company Inc.	
Santa Monica Division	
ATTN: Mr. J. L. Waisman	
Santa Monica, California	1
E. I. DuPont Nemours and Co.	
Eastern Laboratories	
ATTN: Mr. C. P. Williams	1
Mr. J. J. Douglass	1
Wilmington 98, Delaware	
General Electric Company	
Rocket Engine Section	
Flight Propulsion Laboratory Department	
Cincinnati 15, Ohio	1

SUPPLEMENTAL DISTRIBUTION LIST

	No. of Copies
H. I. Thompson Fiber Glass Co. 1600 West 135th Street Gardena, California	1
Kaiser Aluminum & Chemical Corp. Spokane Washington	1
A. D. Little, Inc. ATTN: Dr. R. Davis Acorn Park Cambridge 40, Mass.	1
Ladish Company ATTN: Mr. R. P. Daykin Cudahy, Wisconsin	1
Lyon, Inc. ATTN: Mr. W. Martin 13881 W. Chicago Boulevard Detroit, Michigan	1
Manufacturing Laboratories ATTN: Dr. P. Fopiano Dr. V. Radcliffe 21-35 Erie Street Cambridge 42, Mass.	1 1
Minneapolis-Honeywell Regulator Co. 1230 Soldier Field Road Brighton 35, Mass.	1
Norris-Thermador Corporation ATTN: Mr. L. Shiller 5215 South Boyle Avenue Los Angeles 58, California	1
The Perkin-Elmer Corporation ATTN: Mr. H. L. Sachs Main Avenue Norwalk, Connecticut	1
Pratt & Whitney Aircraft ATTN: Mr. F. A. Crosby East Hartford, Connecticut	1

SUPPLEMENTAL DISTRIBUTION LIST

	No. of Copies
Reactive Metals Corporation ATTN: Mr. H. Lundstrem Niles, Ohio	1
Republic Steel Corporation Research Center ATTN: Mr. H. P. Manger Independence, Ohio	1
Space Technology Laboratories, Inc. ATTN: Technical Information Center Document Procurement Post Office Box 95001 Los Angeles 45, California	1
Thiokol Chemical Corporation Utah Division Brigham City, Utah	1
Thiokol Chemical Corporation Reaction Motors Division Denville, New Jersey	1
Thompson Ramo Wooldridge, Inc. Tapco Group ATTN: W. J. Piper 207 Hindry Avenue Inglewood, California	1
Titanium Metals Corporation ATTN: Mr. G. Erbin 233 Broadway New York, N. Y.	1
Universal-Cyclops Steel Corp. Stewart Street Bridgeville, Pennsylvania	1
U.S. Borax Research Corp. ATTN: Mr. R. J. Brotherton 412 Crescent Way Anaheim, California	1
United States Rubber Company Research Center ATTN: Dr. E. J. Joss Wayne, N. J.	1

SUPPLEMENTAL DISTRIBUTION LIST

	No. of Copies
Wyman-Gordon Company ATTN: Mr. A. Rustay Grafton, Mass.	1
D. Educational Institutions	
Massachusetts Institute of Technology ATTN: Prof. W. A. Backofen Prof. M. C. Flemings Cambridge, Massachusetts	1 1
Mellon Institute ATTN: Dr. H. L. Anthony Mr. C. J. Owen 4400 Fifth Avenue Pittsburgh 13, Pa.	1 1
Michigan State University ATTN: Mr. R. N. Hammer Department of Chemistry East Lansing, Michigan	1
Ohio State University Research Foundation ATTN: Dr. R. McMaster Columbus, Ohio	1